Mutation of D201G near the receptor binding site significantly drive antigenic drift of circulating H9N2 subtype avian influenza virus

Jing Xia[1], Yu-Wen Luo[1], Meng-Yi Dong[1], Yong-Xin Li[1], An-Dong Wang[1], Nian-Ling Li[1], Yu-Xi Shen[1], Shu-Yun Li[1], Min Cui[1], Xinfeng Han[1], Song-Cheng Yu[2], Min Li[3], and Yong Huang[1]

[1]Sichuan Agricultural University - Chengdu Campus
[2]Meishan Dongpo District Agricultural and Rural Burean Livestock station Meishan 620010 Sichuan China
[3]Animal disease prevention and control center of Chengdu city Chengdu 610041 Sichuan China

May 19, 2022

Abstract

The H9N2 subtype of avian influenza virus (H9N2 AIV) has caused significant losses in chicken flocks throughout China. Our previous research has showed that field isolates of H9N2 underwent antigenic drift to evolve into distinct groups with significant antigenic divergence from the commercially available vaccines. The present study sought to identify which single mutations that have naturally appeared in isolates from the past 5 years has driven antigenic drift. Six high-frequency mutation sites in/near the receptor binding site (RBS) region were screened by comparing amino acid alignments of the H9N2 AIVs isolated from China between 2014 and 2019. Two substitutions, (A168N and D201G) were demonstrated to have a significant impact on the antigenicity, but did not change the growth kinetics and cell tropism of the virus. It is worth noting that the D201G substitution not only significantly changed the antigenicity, but also caused immune escape of the parental virus. In conclusion, A168N and D201G substitution are newly discovered determinants that can significantly change the antigenicity of H9N2 AIV, which should be tracked during outbreaks.

Mutation of D201G near the receptor binding site significantly drive antigenic drift of circulating H9N2 subtype avian influenza virus

Short title: Antigenic drift site of H9N2 AIV

Jing Xia[1,2¶], Yu-Wen Luo[1,2¶], Meng-Yi Dong[1,2], Yong-Xin Li[1,2], An-Dong Wang[1,2], Nian-Ling Li[1,2], Yu-Xi Shen[1,2], Shu-Yun Li[1,2], Min Cui[1,2], Xin-Feng Han[1,2], Song-Cheng Yu[3], Min Li[4*], Yong Huang[1,2*]

1. Preventive of Veterinary Medicine, College of Veterinary Medicine, Sichuan Agricultural University, Chengdu 611130, Sichuan, China.

2. Key Laboratory of Animal Disease and Human Health of Sichuan Province, Sichuan Agricultural University, Chengdu 611130, Sichuan, China.

3. Meishan Dongpo District Agricultural and Rural Burean, Livestock station, Meishan 620010, Sichuan, China

4. Animal disease prevention and control center of Chengdu city, Chengdu 610041, Sichuan, China

[¶] These authors contributed equally to this work

* Correspondence:

Yong Huang, E-mail: hyong601@163.com

Min Li, E-mail: 350360849@qq.com

Jing Xia: 14551@sicau.edu.cn xiajing1028@163.com

Yu-Wen Luo: Yuwen_Luo@126.com

Meng-Yi Dong: 18200356764@163.com

Yong-Xin Li: 41984561@qq.com

An-Dong Wang: antone@stu.sicau.edu.cn

Nian-Ling Li: linianling123@163.com

Yu-Xi Shen: shenyuxi1019@163.com

Shu-Yun Li: lishuyun607@163.com

Min Cui: cuimintracy@163.com

Xin-Feng Han: hanxinf@163.com

Song-Cheng Yu: 853769133@qq.com

Summary:

The H9N2 subtype of avian influenza virus (H9N2 AIV) has caused significant losses in chicken flocks throughout China. Our previous research has showed that field isolates of H9N2 underwent antigenic drift to evolve into distinct groups with significant antigenic divergence from the commercially available vaccines. The present study sought to identify which single mutations that have naturally appeared in isolates from the past 5 years has driven antigenic drift. Six high-frequency mutation sites in/near the receptor binding site (RBS) region were screened by comparing amino acid alignments of the H9N2 AIVs isolated from China between 2014 and 2019. Two substitutions, (A168N and D201G) were demonstrated to have a significant impact on the antigenicity, but did not change the growth kinetics and cell tropism of the virus. It is worth noting that the D201G substitution not only significantly changed the antigenicity, but also caused immune escape of the parental virus. In conclusion, A168N and D201G substitution are newly discovered determinants that can significantly change the antigenicity of H9N2 AIV, which should be tracked during outbreaks.

Keywords: Avian influenza virus, H9N2, Antigenic drift, Evolution, RBS, Antigenicity

Introduction

Chickens natural infected with the H9N2 subtype of low pathogenic avian influenza (LPAI) exhibited mild respiratory signs and decreased egg production. Co-infection with other pathogenic microorganisms will aggravate the clinical signs. Although the H9N2 subtype of avian influenza virus (H9N2-AIV) is of low pathogenicity to birds, the actual threat lies in its broad host range. The virus not only infects birds, but has been reported to jump species to infect humans and other mammals. More serious H9N2-AIV frequently donates gene segments to facilitate the generation of novel reassortants, causing epidemics or even pandemics in poultry (Gerloff et al., 2014). An analysis of the hemagglutinin (HA) gene sequence database of the National Center for Biotechnology Information (NCBI) in 2016 revealed that <90% of the H9N2-AIV isolates came from Asia, of which 78% originated in China (Li et al., 2017). Another dataset showed that the AIV positivity rate was 12.73% between 2016 and 2019 in China, of which H9N2 accounted for 72.75% of cases (Bi et al., 2020). This shows that H9N2-AIV has become the dominant AIV in recent years within China, which seriously threatens the public health of humans as well as the livestock and poultry industries.

Vaccination of poultry is a key element of disease control in endemic countries. Influenza A virus mutates rapidly, resulting in antigenic drift and poor year-to-year vaccine efficacy. Commercial vaccine strains

of H9N2 in China, including A/chicken/Shandong/6/96 (SD696), A/chicken/Guangdong/SS/94 (SS) and A/chicken/Shandong/F/98 (F98), were all isolated prior to 2000. Previously, we demonstrated that H9N2 virus isolated from 2013 to 2016 in China underwent antigenic drift to evolve into distinct antigenic groups, and accumulated significant antigenic differences compared with the commercial vaccines (Xia, Cui, et al., 2017). A growing body of research supports these observations (Sun & Liu, 2015). The identification of antigenic sites for monitoring of variants for the development effective vaccines is crucial. More than 46 HA amino acid antigenic sites were identified in H9N2-AIV (T. P. Peacock et al., 2017; Song et al., 2020; Su et al., 2020; Wan et al., 2014; Zhu et al., 2015). Some of those positions are multifunctional, such as the D200N substitution, which also increases replication in chicken embryo fibroblast cells and embryonated chicken eggs (Song et al., 2020). It was reported that N166D also affects the pathogenicity (Jin et al., 2019; T. P. Peacock et al., 2017), and the 220 loop deletion could arise in the field due to immune selection pressure, which also reduces HA stability (T. P. Peacock et al., 2017). However, it is still unknown which single substitution of recent isolates is responsible for the observed antigenic drift.

Although the epitopes of H9N2-AIV are not well characterized, it is known that not all substitutions affect viral antigenicity (T. P. Peacock, Harvey, Sadeyen, Reeve, & Iqbal, 2018). For example, mutations in H3N2 and H1N1 viruses near the receptor binding site (RBS) determine major antigenic changes, but are also affected by mutations to adjacent sites as well (Koel et al., 2013; Lewis et al., 2014; Santos et al., 2019). Interestingly, our previous analyses established a link between high-frequency substitutions and those key antigenic sites of H3N2 viruses (Xia et al., 2020). Therefore, the high-frequency mutation sites near the H9N2-AIV HA RBS protein may be related to the key amino acid sites producing antigenic variation. In this study, we aimed to demonstrate that the single high-frequency mutation site near the RBS could drive antigenic drift of H9N2-AIV circulating in 3 recent years in China.

Material and methods

Viruses, cells, eggs and plasmids

Human embryonic kidney 293T (HEK-293T) cells were obtained from the research center for swine diseases of Sichuan Agricultural University, and Madin-Darby canine kidney (MDCK) cells were obtained from Zigong Center for Disease Control and Prevention of Sichuan province (Zigong CDC). Both cell lines were maintained in Dulbecco's modified Eagle's medium (DMEM) supplemented with 10 % fetal calf serum at 37°C with 5% CO_2. Specific pathogen free (SPF) chicken embryos were obtained from the Beijng Merial Vital Laboratory Animal Technology Co., Ltd (Beijing, China). Avian origin H9N2 virus A/Chicken/Sichuan/CQY/2014 (abbreviated as CQY-2014) was isolated by the author's group in 2014. Viruses were propagated in allantoic cavities of 10-day-old SPF embryonated chicken eggs for 48 hours and stored at -80 °C. The dual-promoter plasmid, pHW2000 was provided by Shanghai Veterinary Research Institute, Chinese Academy of Agricultural Sciences.

Phylogenetic and antigenic site analysis of H9N2 HA gene/protein

Collection of sequence data: The HA gene sequences of H9N2-AIV isolated in recent years (2014-2020) were collected from the Global Initiative on Sharing All Influenza Data (GISAID) platform. A total of 4935 sequences were downloaded. A total of 312 records were removed that were duplicates or had a sequence length < 1600 bp. The remaining sequences used for the subsequent analyses covered 4623 taxa.

Phylogenetic analysis : Due to the large amount of data, we cut down the number of sequence for the construction of phylogenetic tree. Next, up to 70 sequences from collection years with greater than 70 sequences per year were randomly sampled while maintaining all sequences from collection years with less than 70 sequences per year. This was performed to prevent over representation of certain years.

Each taxa was aligned using MUSCLE (v3.8.4) (Edgar, 2004) and the proportion of unique mutations were identified by subclade using Geneious Prime. A time-scaled phylogenetic tree was generated using BEAST (v1.8.4) (Drummond, Nicholls, Rodrigo, & Solomon, 2002; Pybus & Rambaut, 2002; Suchard et al., 2018). Parameter setting of the evolutionary model was performed as previously reported (Xia et al., 2020). Briefly,

a nucleotide GTR + I + Γ4 substitution model was selected, with an uncorrelated log-normal prior molecular clock model over a strict clock, and a non-parametric Bayesican skyline demographic tree (Baele et al., 2012; Baele, Li, Drummond, Suchard, & Lemey, 2013; Drummond, Rambaut, Shapiro, & Pybus, 2005). A total of 50 million Markov Chain Monte Carlo generations were specified for sampling every 10,000 steps, and assessed for sufficient mixing and convergence using tracer (v1.6) after considering the first 10% of samples as burn-in (Rambaut, Drummond, Xie, Baele, & Suchard, 2018). A maximum clade credibility (MCC) tree was generated in treeannotator (v1.8.4) and visualized in figtree (v1.4.3). The specific amino acid mutations of each subclade were also counted by comparing the amino acid sequences in Geneious Prime.

Antigenic site counting : Keyword searches in PubMed, Google Scholar, and China national knowledge internet (CNKI) databases were used to count the number of reported H9N2-AIV antigenic sites (Table S1). The mutation and frequency of antigenic sites in years 2014, 2016, 2018 and 2019-2020 were analyzed using BioAider (v1.334) (Zhou, Qiu, Pu, Huang, & Ge, 2020). To demonstrate that the single high-frequency mutation site near the RBS could drive antigenic drift of H9N2-AIV circulating in three recent years in China, the high-frequency mutation sites in/near the RBS, and the substitution accounting for [?] 20% were selected as the pre-selection substitutions for subsequent antigenicity verification.

Generation of single mutant H9N2-AIVs by reverse genetics

Total RNA extraction and reverse transcription (RT) reactions of CQY-2014 were performed as previously reported (Xia et al., 2016). PCR amplification of the 8 gene fragments (PB2, PB1, PA, NP, NS, M, NA and HA) were carried out using the primers presented in Table S2. PCR products were sequenced by Shanghai Sangong Biological Engineering Technology & Services Co., Ltd. (Shanghai, China). Complete genome sequences were submitted to GenBank under the accession numbers MW493190-MW493196 and MW493229.

For the construction of recombinant plasmids, a classical cloning method was used as previously described (Hoffmann, Stech, Guan, Webster, & Perez, 2001). In brief, the 8 purified complete genome fragments were cloned into the dual-promoter plasmid pHW2000 by homologous recombination, and transformed into *E.coli* TOP10 competent cells. Homologous recombinant primers are presented in Table S2. The linearized pHW2000 plasmid was prepared by PCR amplification using the primers pHW2000F: CCCCCC-CAACTTCGGAGGTC and pHW2000R: AATAACCCGGCGGCCCAAAA. Recombination was performed according to the SE seamless cloning and assembly kit instructions (Beijing Zoman Biotechnology, China). The single pre-selection substitutions were separately introduced into the HA1 gene of the CQY-2014 virus using TaKaRa MutanBEST kit (TaKaRa, Japan) according to the manufacturer's instructions. At least 4 clones were picked for each transformation pool of recombinant plasmid, and was sequenced to ensure the absence of unwanted mutations. Viral rescue was performed by transfecting 293T cells with plasmid prepared using the Lipofectamine^{TM} 3000 Reagent Protocol kit (Thermo Fisher Scientific, China). The supernatant and cell mixture were harvested after 48 h of culture and blind passaged in MDCK cells for 3 generations. Hemagglutination test and RT-PCR were used to identify the rescued viruses.

Replication kinetics in MDCK cells and chicken embryos

Growth properties of rescued mutant and parental viruses were compared in MDCK cells and chicken embryos. Each virus was inoculated onto MDCK monolayers and nine-day old chicken embryos at a multiplicity of infection (MOI) of 0.001 and 10^3EID$_{50}$, respectively. The supernatants of the infected cells and chicken embryos were collected in triplicate at 2, 4, 6, 12, 24, 36, 48 and 72 h post inoculation and stored at -80^{o}C. The titer of each sample was determined using Quantitative real time PCR (qRT-PCR) and HA tests.

Antigenic analysis of mutants

To determine whether high-frequency mutations near the RBS could drive antigenic drift of H9N2-AIV, antiserum preparation and reciprocal HI tests were performed as previously reported (Xia, Cui, et al., 2017). Here, three criteria (antigenic relatedness values (ARV, r) of HI and microneutralization titer, and antigenic map) were used to judge the difference of virul antigenicity.

The HI and microneutralization titers were used to calculate the "r" by the method of Archetti & Horsfall (1950):AVR $(r) = \sqrt{r1 \times r2} \times 100\%$ where r1 represents the ratio of the heterologous HI titer of virus 1 to the homologous titer of virus 1, and r2 represents the ratio of heterologous titer of virus 2 to the homologous titer of virus 2. Mutants where 0.67 [?] r ¡ 1.5 were considered to be antigenically similar, whereas those with 0.5 [?] r ¡ 0.67 were considered to possess small antigenic differences, and r ¡ 0.5 and r [?] 1.5 were considered to contain significant antigenic differences. Antigen mapping were also performed by using the program AntigenMap (http://sysbio.cvm.msstate.edu/AntigenMap) as previously reported (Xia, Cui, et al., 2017).

Sites between non-adjacent unit were considered to have antigenic differences. The farther the distance, the greater the antigenicity difference. The mutation was been considered as significant if they were supported by both of the r value and antigen map.

Analysis of immune protection conferred by the parental strain against single mutants

To identify whether the key antigenic single mutations can break through the immune protection induced by the parental strain, the parental virus CQY-2014 was selected as the vaccine strain and prepared as an oil-adjuvant inactivated vaccine, as previously reported (Xia, Yao, et al., 2017). Commercial un-immunized 28-day-old Partridge Shank broilers (n = 80) were randomly divided into 8 groups, 4 groups were subcutaneously immunized with 10^5EID$_{50}$ CQY-2014 inactivated vaccine. At 21 day-post-immunization (d.p.i), birds of 3 immune-challenge groups and 3 challenge control groups were challenged with 10^6EID$_{50}$ of CQY-2014, CQY-A168N, or CQY-D201G virus by eye and nose drip, respectively. The birds of immune control group were received only the CQY-2014 vaccine. Birds of blank control group were mock infected with phosphate-buffered saline (PBS) buffer at the corresponding time points.

Chicken feeding and sample collection were carried out as previously described (Xia, Cui, et al., 2017). Briefly, birds in each group were held in separate biosafety level 2+ (BSL2+) isolators and monitored daily for appetite, activity, fecal output, conjunctivitis, cyanosis of the comb, ruffled feathers and dyspnea. Tracheal swabs from each group were collected at 3, 5 and 7 day-post-challenge (d.p.c) for virus isolation. At 14 d.p.c, all remaining birds were euthanized and necropsied for pathological observation.

Ethical compliance

All animal experiments were conducted in compliance with protocols approved by the Sichuan provincial Laboratory Animal Management Committee [Permit Number SYXK (Sichuan) 2019-187], and the Ethics and Animal Welfare Committee (EAWC) of the Sichuan Agricultural University. Humane endpoints were strictly adhered to over the entire experimental period. Birds that were unable or unwilling to eat and/or drink during the study period were immediately euthanized. All birds were euthanized via cervical dislocation by a trained technician, as approved by the EAWC.

Results

Phylogenetic analysis

H9N2 AIV isolates evolved at steady mean evolutionary rates, 8.036×10^{-3} (95% HPD: 6.058×10^{-3}˜ 9.702×10^{-3}) in recent years in China. All randomly down-sampling sequences belonged to clade 15 of H9N2-AIV. The sequences were diversified into 3 additional subclades (A, B and C) based on significant nucleotide differences, with subclade C comprising the predominant branch (Figure 1).

Seven high-frequency mutation sites were located near/in RBS

A total of 46 reported antigenic sites were curated form research papers in three databases (Table S1). A total of 2,927 full-length HA sequences were analyzed in this part of the study. Only 43.48% (20/46) of the sequences were hypervariable under the natural selection, most of which were conservative (Table S1). Interestingly, 14 of the 20 mutant antigenic sites (70%) are located in/near the HA RBS.

Figure 1 shows the specific mutations of each additional subclade, consisting of a total of 14 amino acid sites,

which were also distributed in/near the RBS. Of those, 6 positions, including 164, 168, 171, 198, 200 and 201 (H9 numbering) near/in the RBS of H9N2-AIV were selected as high-frequency mutations sites. All of those seven sites were located on the surface of the HA protein head domain (Figure 2A). The seven mutations (R164Q, A168N, I171T, T198A, R200T, D201G and D201A) were selected as the pre-selection substitutions for subsequent antigenicity verification.

Comparison of growth characteristics of the mutants

The virus, CQY-2014, was generated from a wild-type H9N2-AIV using reverse genetics. Each of the high-frequency mutation sites (R164Q, A168N, I171T, T198A, R200T, D201G and D201A) were introduced into the CQY-2014 backbone individually, and there were no unexpected mutations in the sequencing of each virus (Figure 3 A). The titer of the parental CQY-2014 virus in chicken embryos reached 8.5log10 EID_{50}/mL. Observed titers in MDCK cells were slightly lower at 6.5log10 $TCID_{50}$/mL. Compared with the parental virus, titers of the seven mutants were slightly lower in both CEK cells and chicken embryos (Table 1). However, no significant differences among growth curves were observed (Figure 3 B).

Two single substitutions significantly change the antigenicity of H9N2-AIV

A total of seven substitutions (including six high-frequency mutation sites) in/near the RBS were tested using reciprocal HI and microneutralization test to support the hypothesis that the single high-frequency mutation site near the RBS drives antigenic drift of H9N2-AIV. The original data were suppored in Table S3 and Figure S1, and the Integration results were shown in Table 2. As the Table 2 showed, mutations that drive antigen drift were different, whether based on the r-values of HI and neutralizing titers, or the antigen maps. Only two mutations, A168N and D201G were strong supported by all criteria, and those two mutations were considered to significantly cause the antigenic differences. The other 5 mutations, which are only supported by partial criteria, are thought to exerte mild effects on antigenicity. Notably, at the 201 site, two single substitutions (either D to G and D to A) produced drastic phenotypic differences, with glycine (G) had a significant effect on antigenicity, while the substitution of alanine (A) had no significant effect. The visualizations in Figure S1 were even more obvious. The antigen distance between the two single substitutions at site 201 was more than 2 units in antigen map, with more than 4-fold HI and microneutralization titer change. By predicting the 3D structure of the HA protein, it was observed that the substitution of glycine at position 201 did not change the α helix structure, but significantly changed the surface structure (Figure 2 B). In conclusion, the A168N and D201G mutations near the RBS significantly affected the antigenicity of circulating H9N2-AIV.

Immune protection analysis

Next, the ability of the two mutants (A168N and D201G) to break through the immune protection induced by the parent strain was analyzed by avaccinal protection test. There were no unexpected deaths observed during the study in all groups. There was also no infection in immunized control chickens (Vaccine_control group) and blank control group. No significant difference in the proportion of sick chickens with respiratory signs were observed (including cough and mouth breathing) among the 3 challenge control groups (CQY-2014, A168N and D201G group) at 3 ˜ 6 day-post-challenge (d.p.c), which were between 50% ˜ 70%. At 14 d.p.c, the pathological lesions of chickens in each of the 3 challenge and control groups were also similar, and about 20% ˜ 30% of chickens had intestinal and tracheal congestion or hemorrhage. The results suggest that the 2 key mutations (A168N and D201G) influencing antigenicity did not exert a significant effect on H9N2-AIV pathogenicity.

Comparing the data between the 3 immune-challenge groups, it can be observed that the D201G mutation [Vaccine_(D201G) group] has the potential ability to break through the immune protection conferred by the parental virus. Recovery of challenge virus remained at 60% and 20% at 5 and 7 d.p.c, respectively (Figure 4 B and C). During the study 30% of chickens presented with signs of respiratory disease in Vaccine_(D201G) group. Groups challenged with other mutants had a significant decrease in re-isolation rate (20% ˜30%) at 5 d.p.c. At 7 d.p.c., no virus was isolated and no clinical signs or pathological impairments were observed (Figure 4). The results suggested that the D201G mutation not only changes the antigenicity of H9N2-AIV,

but also confers the ability to escape the host immune responses.

Discussion

Avian influenza viruses have posed a significant threat to the global poultry industry, in addition to public health. Due to the wide host range, some H9N2 AIVs not only circulate in poultry and wild bird population, but have also been detected in mammals, and which elevates the risk of transmission to humans. Another concern is the extensive genetic reassortment with other influenza serotypes, with H9N2 AIV considered to be the most common and destructive LPAIV subtype. While vaccination is an effective method to control the spread of influenza viruses, the efficacy of the H9N2 AIV vaccine has been challenged by the perpetual antigenic drift. Our previous research demonstrated that H9N2 field isolates have undergone antigenic drift to evolve into distinct antigenic groups, which also resulted in significant antigenic differences with the commercial vaccines. Unfortunately, the key amino acids associated with those antigenic drift events remain elusive. Two discrete antigenic sites "H9-A" and "H9-B" (or group I and II) which include at least 46 amino acid sites have been identified (T. Peacock et al., 2016). We also analyzed the evolution of these 46 aa in isolates collected over the most recent five years and found that most of these sites were completely conserved among circulating H9N2 viruses. To identify which single mutations of these viruses are driving the antigenic drift, 6 high-frequency mutations including those at aa sites 164, 168, 171, 198, 200 and 201 were screened by comparing amino acid alignments of the H9N2 AIVs isolated from China in 2014-2019. It should be noted that 5 of these (164,168,198,200 and 201) are located both in the antigenic sites and RBS region (Kaverin et al., 2004). Three of them (164, 168 and 201) were under positive selection (data not shown) pressure (Su et al., 2020). Therefore, these sites were likely responsible for the significant antigenic drift observed in recent years.

A variety of mechanisms, namely changes to epitope structure, acquisition of additional glycosylation sites and modulation of receptor-binding avidity, can contribute to both actual and apparent antigenic change (Abe et al., 2004; Das et al., 2011; Hensley et al., 2009). In the present study, 2 sites containing a high-frequency of mutations were identified that contribute to the viral antigenic drift. The A168N and D201G substitutions resulted in significant antigenic changes.

The HA protein of influenza is a highly glycosylated. N-linked glycosylation of HA has been reported to contribute to immune escape and virulence of influenza (Gao et al., 2021), and obtaining new glycosylation sites is also an important mechanism of viral antigenic drift. None of the mutations characterized here introduced novel glycosylation sites into the virus. In response to escape under neutralizing antibody pressure of the virus, influenza A virus could evolve by regulating HA receptor avidity via amino acid substitutions in the HA1 globular head domain (Das et al., 2011), many of which simultaneously alter the antigenicity (Hensley et al., 2009; Wu & Wilson, 2020). Some studies have shown that receptor avidity may be a more important factor than antigenicity in avoiding neutralizing antibodies (Crowe, 2012). Here, the effects of two mutations at antigenic site II of residue 201 (D201G and D201A) on antigenicity were significantly altered, in which the glycine substitution had a significant effect both on antigenicity and immune escape, while alanine had no effect. In addition, a serine substitution at residue 201 can also lead to antibody escape (Wan et al., 2014). It was observed that the change of surface structure was a result of the D201G substitution (G: hydrophobic, D: hydrophilic). This in turn may be due to the change of hydrophilicity, thus leading to the change of receptor avidity and antigenicity of the virus. It is important to note that changes in receptor avidity were not validated at residue 201 in this study. Of note, 201G mainly exists in predominant subclade C (Figure 1), which may result in immune escape in chicken flocks in the future. The other sites that may cause a similar phenomenon are at residues 201 and 168, which are both in the antigenic epitopes and RBS region. It was observed that asparagine (N, 37.1%) and alanine (A, 35.7%) accounted for the largest proportion at residue 168 in 2019-2020, which was significantly different from the major site (aspartic acid, D, 52.9%, and A, 33.0%) in 2014 by amino acid comparisons (Table S1). The substitution of those three amino acids can affect the antigenicity of H9N2 viruses (T. Peacock et al., 2016).

Comprised of a weak genetic basis of preferences for alternative avian receptors and human-like receptors, residue 198 may be a multifunctional site which could function to modulate polyclonal antisera binding and

receptor-binding avidity at the same time (T. P. Peacock et al., 2020). In the present study, T198A was capable of immune escape in a reciprocal HI assay using polyclonal antibodies, while escape was not observed in a microneutralization assay. One possible explanation for this result is that the HI receptor-binding avidity and neutralization antibody epitopes are different. Thus, the molecular basis requires an in depth analysis, which is beyond the scope of this report.

In conclusion, key amino acid substitutions that may drive antigenic drift of H9N2-AIV in a recent five year periods were identified. Two predominant substitutions, including A168N and D201G were demonstrated to significantly affect antigenicity, but did not change growth characteristics and cell tropism. It is worth noting that the D201G substitution not only changed the antigenicity, but also produced an immune escape variant of the parental virus. The data presented here provide a reference for the prediction of the evolutionary direction of H9N2-AIV, and the development of effective vaccines.

Acknowledgements

This work was financially supported by the Program of "Shuangzhi plan" of Sichuan Agriculture University.

Conflict of interest statement

All authors have no conflict of interest to declare.

Reference

Abe, Y., Takashita, E., Sugawara, K., Matsuzaki, Y., Muraki, Y., & Hongo, S. (2004). Effect of the addition of oligosaccharides on the biological activities and antigenicity of influenza A/H3N2 virus hemagglutinin. J Virol, 78(18), 9605-9611. doi:10.1128/JVI.78.18.9605-9611.2004

Baele, G., Lemey, P., Bedford, T., Rambaut, A., Suchard, M. A., & Alekseyenko, A. V. (2012). Improving the accuracy of demographic and molecular clock model comparison while accommodating phylogenetic uncertainty. Mol Biol Evol, 29(9), 2157-2167. doi:10.1093/molbev/mss084

Baele, G., Li, W. L., Drummond, A. J., Suchard, M. A., & Lemey, P. (2013). Accurate model selection of relaxed molecular clocks in bayesian phylogenetics. Mol Biol Evol, 30(2), 239-243. doi:10.1093/molbev/mss243

Bi, Y., Li, J., Li, S., Fu, G., Jin, T., Zhang, C., . . . Shi, W. (2020). Dominant subtype switch in avian influenza viruses during 2016-2019 in China. Nat Commun, 11(1), 5909. doi:10.1038/s41467-020-19671-3

Crowe, J. E., Jr. (2012). Influenza virus resistance to human neutralizing antibodies. mBio, 3(4), e00213-00212. doi:10.1128/mBio.00213-12

Das, S. R., Hensley, S. E., David, A., Schmidt, L., Gibbs, J. S., Puigbo, P., . . . Yewdell, J. W. (2011). Fitness costs limit influenza A virus hemagglutinin glycosylation as an immune evasion strategy. Proc Natl Acad Sci U S A, 108(51), E1417-1422. doi:10.1073/pnas.1108754108

Drummond, A. J., Nicholls, G. K., Rodrigo, A. G., & Solomon, W. (2002). Estimating mutation parameters, population history and genealogy simultaneously from temporally spaced sequence data. Genetics, 161(3), 1307-1320. doi:10.1093/genetics/161.3.1307

Drummond, A. J., Rambaut, A., Shapiro, B., & Pybus, O. G. (2005). Bayesian coalescent inference of past population dynamics from molecular sequences. Mol Biol Evol, 22(5), 1185-1192. doi:10.1093/molbev/msi103

Edgar, R. C. (2004). MUSCLE: multiple sequence alignment with high accuracy and high throughput. Nucleic Acids Res, 32(5), 1792-1797. doi:10.1093/nar/gkh340

Gao, R., Gu, M., Shi, L., Liu, K., Li, X., Wang, X., . . . Liu, X. (2021). N-linked glycosylation at site 158 of the HA protein of H5N6 highly pathogenic avian influenza virus is important for viral biological properties and host immune responses. Vet Res, 52(1), 8. doi:10.1186/s13567-020-00879-6

Gerloff, N. A., Khan, S. U., Balish, A., Shanta, I. S., Simpson, N., Berman, L., . . . Davis, C. T. (2014). Multiple reassortment events among highly pathogenic avian influenza A(H5N1) viruses detected in Bangladesh. Virology, 450-451, 297-307. doi:10.1016/j.virol.2013.12.023

Hensley, S. E., Das, S. R., Bailey, A. L., Schmidt, L. M., Hickman, H. D., Jayaraman, A., . . . Yewdell, J. W. (2009). Hemagglutinin receptor binding avidity drives influenza A virus antigenic drift. Science, 326(5953), 734-736. doi:10.1126/science.1178258

Hoffmann, E., Stech, J., Guan, Y., Webster, R. G., & Perez, D. R. (2001). Universal primer set for the full-length amplification of all influenza A viruses. Arch Virol, 146(12), 2275-2289. doi:10.1007/s007050170002

Jin, F., Dong, X., Wan, Z., Ren, D., Liu, M., Geng, T., . . . Ye, J. (2019). A Single Mutation N166D in Hemagglutinin Affects Antigenicity and Pathogenesis of H9N2 Avian Influenza Virus. Viruses, 11(8). doi:10.3390/v11080709

Kaverin, N. V., Rudneva, I. A., Ilyushina, N. A., Lipatov, A. S., Krauss, S., & Webster, R. G. (2004). Structural differences among hemagglutinins of influenza A virus subtypes are reflected in their antigenic architecture: analysis of H9 escape mutants. J Virol, 78(1), 240-249. doi:10.1128/jvi.78.1.240-249.2004

Koel, B. F., Burke, D. F., Bestebroer, T. M., van der Vliet, S., Zondag, G. C., Vervaet, G., . . . Smith, D. J. (2013). Substitutions near the receptor binding site determine major antigenic change during influenza virus evolution. Science, 342(6161), 976-979. doi:10.1126/science.1244730

Lewis, N. S., Anderson, T. K., Kitikoon, P., Skepner, E., Burke, D. F., & Vincent, A. L. (2014). Substitutions near the hemagglutinin receptor-binding site determine the antigenic evolution of influenza A H3N2 viruses in U.S. swine. J Virol, 88(9), 4752-4763. doi:10.1128/JVI.03805-13

Li, X., Tian, B., Jianfang, Z., Yongkun, C., Xiaodan, L., Wenfei, Z., . . . Shu, Y. (2017). A comprehensive retrospective study of the seroprevalence of H9N2 avian influenza viruses in occupationally exposed populations in China. PLoS One, 12(6), e0178328. doi:10.1371/journal.pone.0178328

Okamatsu, M., Sakoda, Y., Kishida, N., Isoda, N., & Kida, H. (2008). Antigenic structure of the hemagglutinin of H9N2 influenza viruses. Arch Virol, 153(12), 2189-2195. doi:10.1007/s00705-008-0243-2

Peacock, T., Reddy, K., James, J., Adamiak, B., Barclay, W., Shelton, H., & Iqbal, M. (2016). Antigenic mapping of an H9N2 avian influenza virus reveals two discrete antigenic sites and a novel mechanism of immune escape. Sci Rep, 6, 18745. doi:10.1038/srep18745

Peacock, T. P., Benton, D. J., James, J., Sadeyen, J. R., Chang, P., Sealy, J. E., . . . Iqbal, M. (2017). Immune Escape Variants of H9N2 Influenza Viruses Containing Deletions at the Hemagglutinin Receptor Binding Site Retain Fitness In Vivo and Display Enhanced Zoonotic Characteristics. J Virol, 91(14). doi:10.1128/JVI.00218-17

Peacock, T. P., Harvey, W. T., Sadeyen, J. R., Reeve, R., & Iqbal, M. (2018). The molecular basis of antigenic variation among A(H9N2) avian influenza viruses. Emerg Microbes Infect, 7(1), 176. doi:10.1038/s41426-018-0178-y

Peacock, T. P., Sealy, J. E., Harvey, W. T., Benton, D. J., Reeve, R., & Iqbal, M. (2020). Genetic determinants of receptor-binding preference and zoonotic potential of H9N2 avian influenza viruses. J Virol. doi:10.1128/JVI.01651-20

Poh, Z. W., Wang, Z., Kumar, S. R., Yong, H. Y., & Prabakaran, M. (2020). Modification of neutralizing epitopes of hemagglutinin for the development of broadly protective H9N2 vaccine. Vaccine, 38(6), 1286-1290. doi:10.1016/j.vaccine.2019.11.080

Pybus, O. G., & Rambaut, A. (2002). GENIE: estimating demographic history from molecular phylogenies. Bioinformatics, 18(10), 1404-1405. doi:10.1093/bioinformatics/18.10.1404

Rambaut, A., Drummond, A. J., Xie, D., Baele, G., & Suchard, M. A. (2018). Posterior Summarization in Bayesian Phylogenetics Using Tracer 1.7. Syst Biol, 67(5), 901-904. doi:10.1093/sysbio/syy032

Santos, J. J. S., Abente, E. J., Obadan, A. O., Thompson, A. J., Ferreri, L., Geiger, G., . . . Perez, D. R. (2019). Plasticity of Amino Acid Residue 145 Near the Receptor Binding Site of H3 Swine Influenza A Viruses and Its Impact on Receptor Binding and Antibody Recognition. J Virol, 93(2). doi:10.1128/JVI.01413-18

Song, J., Wang, C., Gao, W., Sun, H., Jiang, Z., Wang, K., . . . Pu, J. (2020). A D200N hemagglutinin substitution contributes to antigenic changes and increased replication of avian H9N2 influenza virus. Vet Microbiol, 245, 108669. doi:10.1016/j.vetmic.2020.108669

Su, H., Zhao, Y., Zheng, L., Wang, S., Shi, H., & Liu, X. (2020). Effect of the selection pressure of vaccine antibodies on evolution of H9N2 avian influenza virus in chickens. AMB Express, 10(1), 98. doi:10.1186/s13568-020-01036-0

Suchard, M. A., Lemey, P., Baele, G., Ayres, D. L., Drummond, A. J., & Rambaut, A. (2018). Bayesian phylogenetic and phylodynamic data integration using BEAST 1.10. Virus Evol, 4(1), vey016. doi:10.1093/ve/vey016

Sun, Y., Cong, Y., Yu, H., Ding, Z., & Cong, Y. (2021). Assessing the effects of a two-amino acid flexibility in the Hemagglutinin 220-loop receptor-binding domain on the fitness of Influenza A(H9N2) viruses. Emerg Microbes Infect, 10(1), 822-832. doi:10.1080/22221751.2021.1919566

Sun, Y., & Liu, J. (2015). H9N2 influenza virus in China: a cause of concern. Protein Cell, 6(1), 18-25. doi:10.1007/s13238-014-0111-7

Wan, Z., Ye, J., Xu, L., Shao, H., Jin, W., Qian, K., . . . Qin, A. (2014). Antigenic mapping of the hemagglutinin of an H9N2 avian influenza virus reveals novel critical amino acid positions in antigenic sites. J Virol, 88(7), 3898-3901. doi:10.1128/JVI.03440-13

Wu, N. C., & Wilson, I. A. (2020). Structural Biology of Influenza Hemagglutinin: An Amaranthine Adventure. Viruses, 12(9). doi:10.3390/v12091053

Xia, J., Adam, D. C., Moa, A., Chughtai, A. A., Barr, I. G., Komadina, N., & MacIntyre, C. R. (2020). Comparative epidemiology, phylogenetics, and transmission patterns of severe influenza A/H3N2 in Australia from 2003 to 2017. Influenza Other Respir Viruses, 14(6), 700-709. doi:10.1111/irv.12772

Xia, J., Cui, J. Q., He, X., Liu, Y. Y., Yao, K. C., Cao, S. J., . . . Huang, Y. (2017). Genetic and antigenic evolution of H9N2 subtype avian influenza virus in domestic chickens in southwestern China, 2013-2016. PLoS One, 12(2), e0171564. doi:10.1371/journal.pone.0171564

Xia, J., He, X., Yao, K. C., Du, L. J., Liu, P., Yan, Q. G., . . . Huang, Y. (2016). Phylogenetic and antigenic analysis of avian infectious bronchitis virus in southwestern China, 2012-2016. Infect Genet Evol, 45, 11-19. doi:10.1016/j.meegid.2016.08.011

Xia, J., Yao, K. C., Liu, Y. Y., You, G. J., Li, S. Y., Liu, P., . . . Huang, Y. (2017). Isolation and molecular characterization of prevalent Fowl adenovirus strains in southwestern China during 2015-2016 for the development of a control strategy. Emerg Microbes Infect, 6(11), e103. doi:10.1038/emi.2017.91

Zhou, Z. J., Qiu, Y., Pu, Y., Huang, X., & Ge, X. Y. (2020). BioAider: An efficient tool for viral genome analysis and its application in tracing SARS-CoV-2 transmission. Sustain Cities Soc, 63, 102466. doi:10.1016/j.scs.2020.102466

Zhu, Y., Yang, D., Ren, Q., Yang, Y., Liu, X., Xu, X., . . . Liu, X. (2015). Identification and characterization of a novel antigenic epitope in the hemagglutinin of the escape mutants of H9N2 avian influenza viruses. Vet Microbiol, 178(1-2), 144-149. doi:10.1016/j.vetmic.2015.04.012

Table 1 The titer of mutant CQY-2014 H9N2-AIVs in MDCK cells and chicken embryos

Virus	$TCID_{50}$/mL (log10)	EID_{50}/mL (log10)
Parental virus CQY-2014	6.50	8.50
R164Q	6.0	7.5
A168N	5.33	7.5
I171T	5.0	8.0
T198A	5.0	7.75
R200T	5.0	7.5
D201G	5.33	7.25
D201A	5.33	7.0

Table 2 Analysis of mutants with antigenicity differences compared with parental virus CQY-2014

Influence extent	Judgment method	Judgment method	Judgment method
	r value of HI titer	Antigen map of HI titer	r value of microneut
Significant antigenic differences	**A168N,** T198A, **D201G**	**A168N**, **D201G**	R164Q, **D201G**, **A**
Small antigenic differences	D201A, R164Q	/	I171T, R200T
Antigenically similar	I171T, R200T	T198A, I171T, R200T, D201A, R164Q	T198A

Note: The mutants in bold were those that meet the all criteria

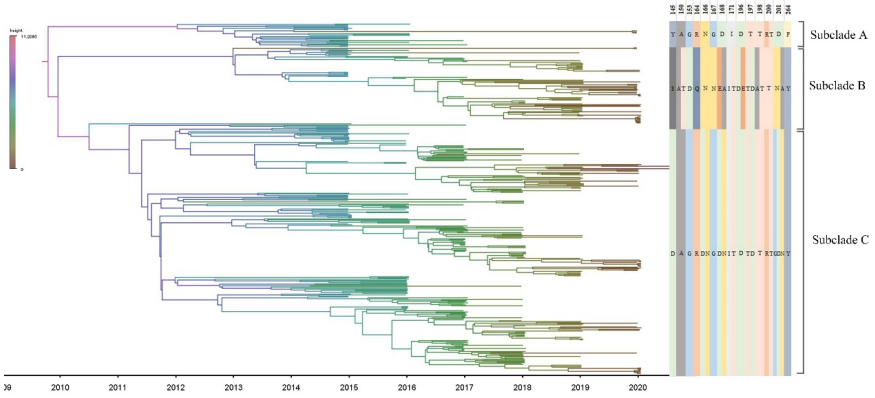

Figure 1 HA maximum clade credibility (MCC) phylogenetic tree and specific antigenic sites for each subclade of H9N2 AIVs isolated between 2014 and 2020 in China. Branches were colored by height. Only specific antigenic mutations accounting for more than 30% of each subclade are presented.

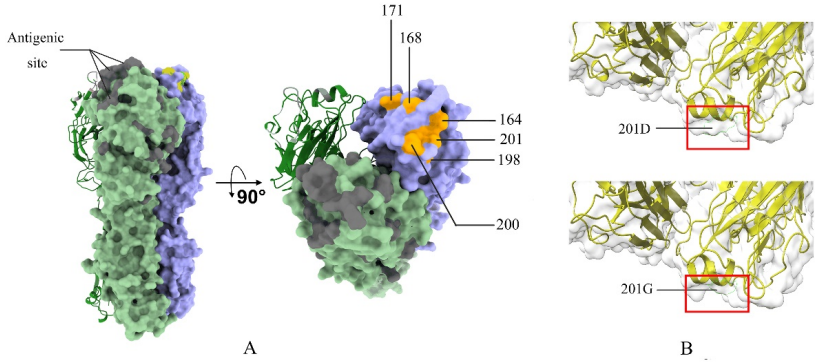

Figure 2 Antigenic sites on the surface of the HA protein of H9N2 AIV. The HA amino acid sequence of CQY-2014 isolate and mutations were uploaded to the SWISS-MODEL website for model prediction, and the predicted trimeric proteins were annotated using the ChimeraX 1.3 software. **A:** Forty-six antigenic sites were labeled gray in the α-subunits, and the six preselected high-frequency mutation sites were labeled yellow in the β-subunits.**B:** When asparagine was substituted with glycine at site 201 (D201G), the α helix structure remained unchanged, but the surface structure changed significantly (red boxes).

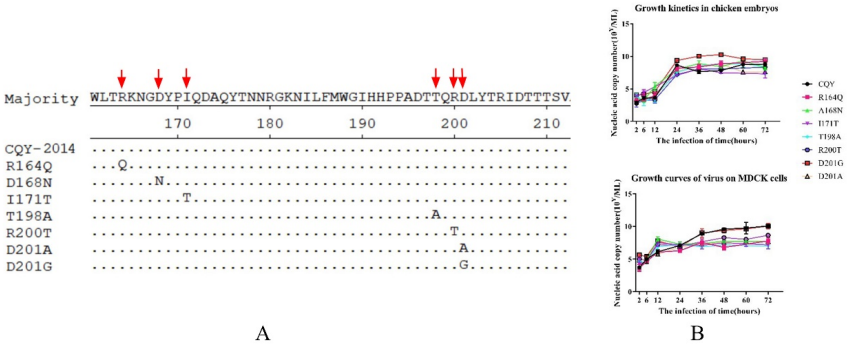

Figure 3 Nucleotide alignment of mutant fragments and growth kinetics of CQY-2014 mutants. **A** : There were no unexpected mutations in the sequencing of each virus. **B** : growth kinetics of CQY-2014 mutants in MDCK cells and chicken embryos.

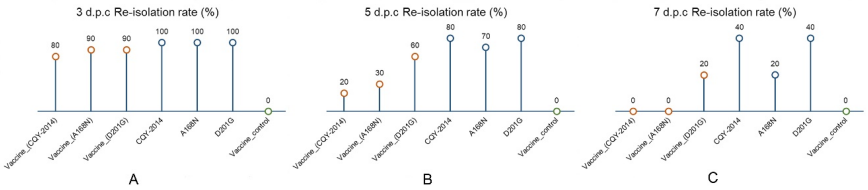

Figure 4 Virus recovery from chickens at different times post challenge.